# Allene Trifluoroacetoxylation with a 2-Phosphinoimidazole-Derived Bimetallic Rh(II) Catalyst

Kelton G. Forson, Rachel N. Owens, Jacob A Parkman, Benjamin O. Bohman, Coriantumr Z. Wayment, Caitlyn E. McKnight, Rhen C. Davis, Lillian R. Stillwell, Kamahao Kini-Lopes, Rebecca J. Cole, Artem Marchenko, Stacey J. Smith, David J. Michaelis[a]*

[a]Department of Chemistry and Biochemistry, Brigham Young University, Provo, UT 84602, USA.

*KEYWORDS Catalysis, hydrofunctionalization, allene, bimetallic catalysis, rhodium*

**ABSTRACT:** We report that a 2-phosphinoimidazole-scaffolded bimetallic Rh(II) complex enables the addition of trifluoroacetic acid across an allene under conditions where monometallic Rh(I) or bimetallic Rh(II) tetracarboxylate catalysts fail. The resulting allyl trifluoroacetate products are isolated in good yield across a range of allene substrates. Mechanistic studies suggest that reversible hydrometallation of the allene is followed by reductive elimination of the trifluoroacetate, which only occurs with our bimetallic catalyst. Monometallic catalyst undergo beta-hydride elimination to give an isomerized diene as the only product rather than undergo the kinetically slow C–O reductive elimination. DFT studies suggest that the barrier for C–O reductive elimination is much lower in the case of the our bimetallic catalyst due to electron-sharing and substrate coordination across both metal centers in the transition state. These studies help explains why the otherwise kinetically disfavored reductive elimination is only observed with our bimetallic catalyst (and not with monometallic Rh catalysts) to give the more thermodynamically stable allylic trifluoroacetate over the isomerized diene product.

Allene hydrofunctionalization is an attractive method for generating new C–C, C–N, and C–O bonds because of the ease of adding a variety of nucleophiles across either of the two alkenes in the allene. [1] In general, the allene functional group reacts faster than the corresponding alkenes or alkynes and the resulting allyl-substituted products can serve as useful intermediates in synthesis. Allenes can be readily accessed by homologation of the corresponding alkyne[2] and this sequence of transformations that includes alkyne homologation and hydrofunctionalization enables access to highly versatile allylic functional groups. This approach compliments work in the development of allylic C-H functionalization reactions.[3] Allene hydrofunctionalization reactions are known to occur with Ag, Au, Rh, and Pd catalysts, yet typically require the use of good nucleophiles such as amines, alcohols, or malonates to achieve high reactivity.[1]

Few examples of allene hydrofunctionalization exist that enable direct installation of a good leaving group that is amenable to additional functionalization through metal-catalyzed pi allyl formation.[1] This limitation is attributed in many cases to kinetically slow C–X bond reductive elimination.[4] Yamamoto[5] and Krische[6] have reported allene hydrocarboxylations under Pd and Ir catalysis, respectively, Breit and coworkers demonstrated the enantioselective addition of carboxylic acid nucleophiles to allenes under Rh catalysis (Figure 1a), and more recently with Ru catalysts.[7] Breit also reported the observation of trifluoroacetate addition products as intermediates for additions of carbon nucleophiles to internal allenes (Figure 1b).[8] In this report, we demonstrate that a newly discovered 2-phosphinoimidazole-derived bimetallic Rh(II) catalyst enables efficient addition of trifluoroacetic acid, a weak nucleophile, across terminal allenes in good yield and with high regioselectivity for the branched allylic trifluoroacetate (Figure 1c). Importantly, monometallic and other bimetallic $Rh_2(CO_2R)_4$ catalysts do not generate the hydrofunctionalization product under our optimized conditions, highlighting the unique reactivity of our new catalyst. DFT studies also demonstrate that the

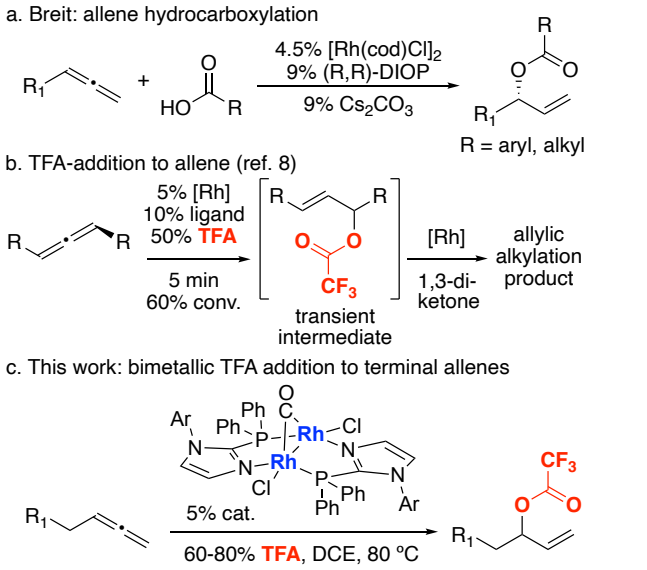


**Figure 1.** a) Allene hydrocarboxylation with Rh catalysts. b) Precedent for trifluoroacetate addition to allenes. c) Trifluoroacetate additions to allenes presented in this work.

reductive elimination with our bimetallic catalyst involves binding of the allyl intermediate across both metal centers, which likely lowers the transition state energy by electron-sharing with both metals.

One important pursuit in our laboratory is the discovery of new reactions and mechanisms via catalysis with hetero- and homobimetallic metal complexes.[9] Our hypothesis is that new mechanisms can result from reactions with metal–metal bonds, via activation of a substrate across both metals, or by accessing uncommon metal oxidation states as part of organometallic mechanisms.[10] Previously, we reported the synthesis of homobimetallic Pd(I) and Pd(II) complexes scaffolded on 2-phosphinoimidazole ligands. These bimetallic complexes enable a new naphthalene synthesis reaction by accessing dimeric Pd(III) intermediates in catalysis.[11] We also demonstrated that the oxidation state of the Pd dimer (Pd(I) vs Pd(II)) can have a dramatic impact on catalysis in Buchwal-Hartwig amination and aminocarbonylation reactions.[12] In an attempt to expand the applications of these ligands to bimetallic catalysis, we attempted the synthesis of the corresponding Rh complexes. When 2-phosphinoimidazole ligand **1** was reacted with $[Rh(cod)Cl]_2$, monometallic complex **2** was formed (Figure 2a). The crystal structure of **2** shows only phosphine binding, which suggests that coordination of both the P and the N of the 2-phosphinoimidazole is unfavorable due to a non-

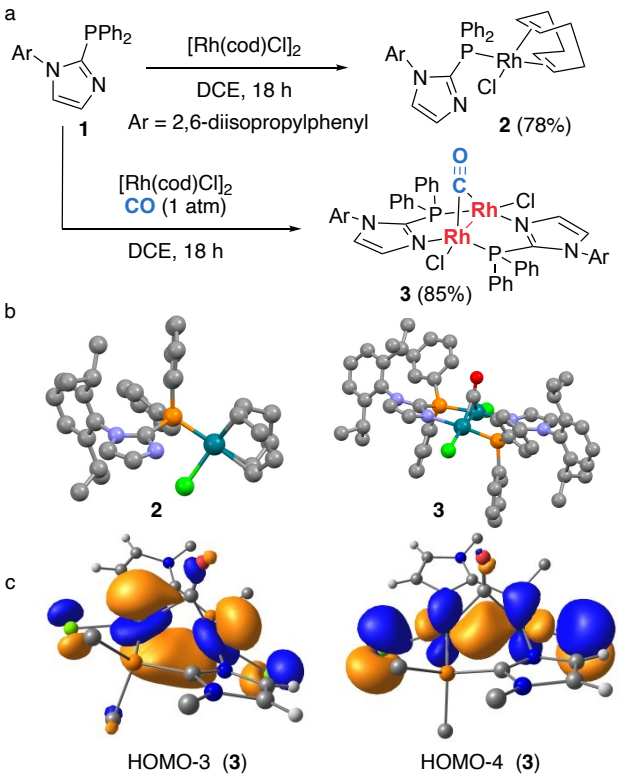


**Figure 2.** a) Synthesis of mono and bimetallic Rh phosphinoimidazole complexes. b) X-ray crystal structures of **1** and **2**. c) Selected Kohn–Sham orbitals (BP86/6-311G(d,p)) for the computationally optimized structure of **3** (*P*-aryl and *N*-aryl substituents of **3** were removed for clarity). d) Reactivity of monometallic and bimetallic Rh complexes with allene substrates.

ideal bite angle (Figure 2b). When the reaction of **1** with $[Rh(cod)Cl]_2$ was run in methanol, however, a trace amount of bimetallic complex **3** was observed, presumably via methanol oxidation. When the same reaction was performed in DCE solvent and under an atmosphere of CO, bimetallic complex **3** could be isolated in excellent yield by precipitation from 1,2-dichloroethane by slow addition of hexanes (98 % yield). No bimetallic complex is observed in the absence of a CO ligand under the same conditions.

The X-ray crystal structure of **3** shows the presence of a bridging CO ligand, which we believe necessary for formation of the bimetallic complex. We believe that coordination of a bridging CO ligand allows the two rhodium centers to achieve a suitable distance on the ligand framework to form a stable complex. The Rh-Rh bond distance for complex **3** is 2.6227 Å, and the formal shortness ratio (FSR) of the Rh-Rh bond is 1.05.[13] These data suggest that the metals are in close enough proximity to form a Rh-Rh bond, wherein the CO ligand would serve as a "ketone-like" ligand and not form a 2-electron, 3-center bond.[14] This would suggest that the CO ligand facilitates formation of high-spin Rh centers, which enables M–M bond formation by creating unpaired electrons at each metal.[15] DFT computed Kohn-Sham orbitals also support the formation of a metal-metal bond (Figure 2c).[16–17] The HOMO-3 and HOMO-4 orbitals of **3** show shared electron density between the two metals, supporting our hypothesis that complex **3** contains a metal–metal bonding interaction.

When exploring the reactivity of our new bimetallic Rh catalyst **3**, we found that **3** readily catalyzes the intramolecular hydroamination reaction to form five, six, and select seven-membered rings (Figure 3a).[7b] In exploring additional hydroamination reactions with substrates that would form larger rings (**4**), we found that no cyclization occurred, but that trifluoroacetic acid was added across the allene to give the allyl trifluoroacetate product **5** (Figure 3b).[7b] This transformation represents a rare example of addition of weak nucleophiles to allenes.[1, 5–8] While trifluoroacetates can be prepared by acetylation of the corresponding alcohol with trifluoroacetic anhydride, this approach enables access to

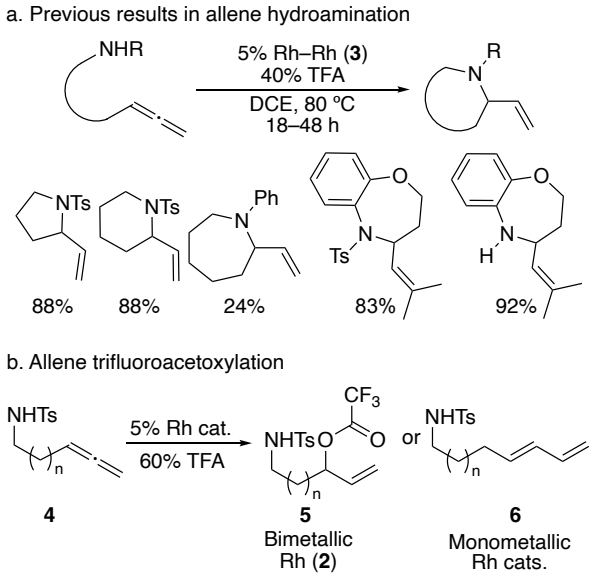


**Figure 3.** a) Allene hydroamination with catalyst **3**. b) Divergent reactivity of bimetallic vs monometallic catalysts.

allylic electrophiles from allenes via C-O bond formation. Allyl trifluoroacettes have also found application as electrophiles in metal-catalyzed C-C bond forming reactions.[18] Importantly, other monometallic Rh(I) and bimetallic Rh(II) complexes either give no reaction or facilitate isomerization to the corresponding diene product **6** (*vide infra*).

Based on the unique ability of our bimetallic Rh complex to facilitate TFA additions to allenes, we performed further optimization studies with substrate **4a** to enhance product formation (Table 1). We first investigated how the amount of TFA added to the reaction would affect the conversion to product **5** (entries 1–5). We found that consumption of starting material was complete with as little as 65% TFA in the reaction. When 1 equiv. TFA was used to try and maximize product yield (entry 5), significant decomposition of starting material was observed and the yield of the reaction decreased. We found that between 60–80% TFA was ideal to provide the highest isolated yield of the TFA addition product (entry 4). We also explored other reaction temperatures (entries 6–7) and solvents (entry 8) and found that running the reaction at 80 °C in dichloroethane (DCE) provide the highest yield of the trifluoroacetate product. We also screened a variety of other Rh(I) catalysts and found

**Table 1.** Optimization of trifluoroacetate addition reaction.

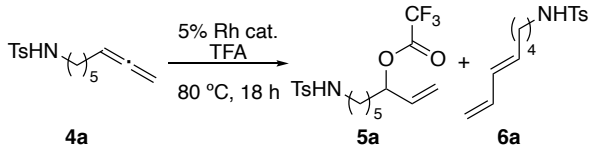


| entry[a] | % cat. | % acid | conv. to **5a**[b] |
|---|---|---|---|
| 1 | 3 | 0 | 0% |
| 2 | 3 | 15 | 15% |
| 3 | 3 | 45 | 90% |
| 4 | 3 | 65 | 100% (64)[c] |
| 5 | 3 | 100 | 100% (50)[c] |
| 6[d] | 3 | 65 | 62% |
| 7[e] | 3 | 65 | 24% |
| 8[f] | 3 | 65 | 83% |
| 9 | **3** (2.5%) | 65 | 57% |
| 10 | **3** (1%) | 65 | 15% |
| 11 | $[Rh(cod)cl]_2$ + dppf | 65 | 100% (**6a**)[g] |
| 12 | $[Rh(cod)cl]_2$ + (R)-SEGPHOS DTBM | 65 | 100% (**6a**)[g] |
| 13 | $Rh(BINAP)(cod)ClO_4$ | 65 | 100% (**6a**)[g] |
| 14 | $Rh_2(OAc)_4$ | 65 | 0% |
| 15 | $Rh_2(5S\text{-}MEPY)_4$ | 65 | 0% |

[a] a) Reaction run on a 0.2 mmol scale of 4 with 5 mol% Rh dimer 3 and the indicated amount of TFA in dichloroethane (DCE, 0.2 M) at 80 ºC for 18 h unless otherwise noted. b) Conversions determined by $^1H$ NMR analysis of the crude reaction mixture by comparing product formed to remaining starting material. c) Isolated yields in parentheses based on amount of allene starting material employed). d) run at 50 °C. e) Run at 23 °C. f) Run in toluene. g) Represents conversion to diene product **5a**.

that in all cases, no TFA addition product was observed. With monometallic Rh(I) complexes, the starting material allene was converted to the isomerized diene product **5a** (entries 11–13). Bimetallic $Rh_2(CO_2R)_4$ catalysts were also screened but no reactivity was observed (entries 14, 15).[19] These final results confirm the unique reactivity of our bimetallic catalyst for addition of weak nucleophiles across allenes.

We next investigated the efficiency of our TFA addition catalyst with a variety of amine-containing substrates originally designed to enable cyclization. Importantly, the yield for each substrate was calculated based on the amount of allene employed to reflect the true synthetic value of the process, rather than calculating the yield based on the amount of limiting reagent (trifluoroacetic acid) used in the reaction. As seen in Figure 4, trifluoroacetate addition to the allene is the main product with a variety of protected sulfonamide (**5a**–**5l**), carbamate (**5n**–**5t**), aniline (**5y**–**5aa**), and amide-containing substrates (**5m**, **5ac**, **5ad**). In all cases, the regioselectivity for formation of the branched

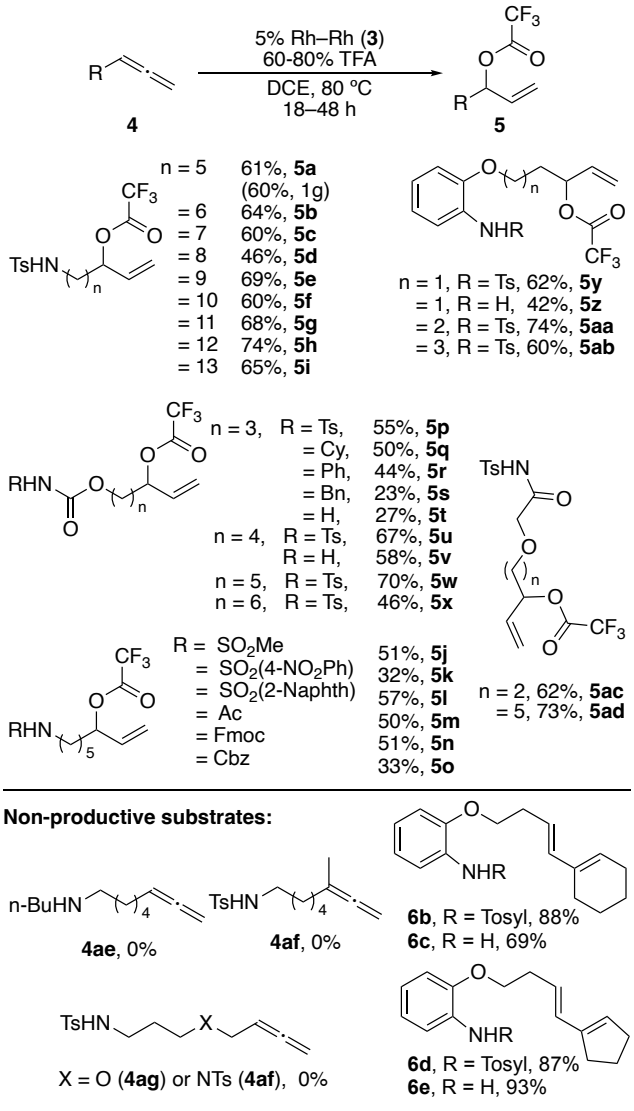


**Figure 4.** Substrate scope and limitations for allene trifluoroacetic acid addition.

secondary allylic trifluoroacetate product was >10:1. Substrates that failed to provide any of the trifluoroacetate product include substrates containing basic amines (**3b**), more hindered 3,3-disubstituted allenes (**3c**), and substrates containing electron-withdrawing heteroatoms at the allenic position (**3d**, **3e**). We also found that certain substrates containing 1,1,3-trisubstituted allenes favored formation of the elimination product to give the corresponding 1,3-diene (**6b**–**6e**). Substrates without amide or sulfonamide groups do react in this transformation (e.g. 1-octene), but are generally isolated in lower yield (<40%) because they appear to be less stable to chromatography.

To further understand the mechanism of TFA addition with catalyst **2**, we next conducted the reaction with TFA-D and deuterated substrate **3a-D** (Figure 5a). As observed previously by Breit,[7b] we found that deuterium incorporation occurred at all carbons of the allene. This result provides evidence for reversible hydrometallation of the allene to form a metal allyl intermediate. A proposed catalytic cycle for TFA addition to allenes based on our observations is shown in Figure 5b. Initial oxidative addition of bimetallic complex **3** into the O–H bond of TFA can generate either **A** or **B**,

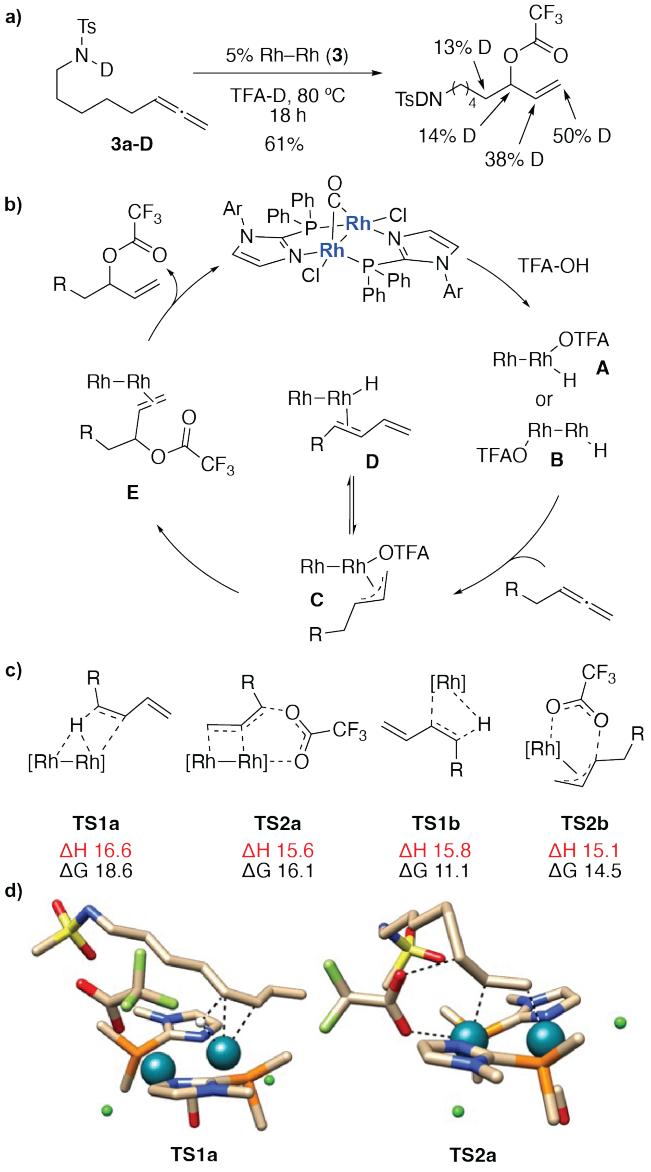


**Figure 5.** a) Mechanistic study and b) proposed mechanism. c) DFT transition states and energies for bimetallic **3** (truncated where Ar = Me) and monometallic [(BINAP)Rh(allyl)(OTFA)] reductive elimination vs beta-hydride elimination. d) DFT-calculated transition states **TS1a** and **TS2a**. (basis set = 6-31g(d,p) [Rh,lanl2dz]).

depending on whether oxidative addition occurs across one or both metals. Subsequent reversible Rh-hydride insertion into the allene then provides intermediate **C**. Intermediate **C** could then either undergo β-hydride elimination to give the diene (as with monometallic Rh(I) complexes) or undergo reductive elimination to form the new C–O bond. Reductive elimination and C–O bond formation gives intermediate **E**, and loss of product then regenerates **3**. For all of the monometallic Rh(I) catalysts tested, the diene product observed results from β-hydride elimination at allyl intermediate **C** to give **D** and no reductive elimination product **E** is observed.

To further elucidate the selectivity of our bimetallic Rh complex **3** vs monometallic Rh(I) complexes, we performed DFT calculations[16–17] of key catalytic steps that determine selectivity between the trifluoroacetate product (**5**) and the diene (**6**). We first calculated the barriers for various possible reductive elimination vs beta hydride elimination steps for a simplified structure of our bimetallic catalyst **3** (Figure 5c, aryl rings replaced with methyl groups on **3**). We found that the barrier for beta hydride elimination from **C** to **D** (TS1a) was 2.5 kcal/mol higher in energy than the corresponding barrier for reductive elimination of TFA to form product **E** (TS2a). This result supports our hypothesis as to why an otherwise kinetically slow reductive elimination is favored with bimetallic catalyst **3**. Figure 5d shows the computed structures for the reductive elimination (TS1a) and beta-hydrogen elimination (TS2a) transition states with catalyst **3**. Interestingly, the formation of a bridging allyl ligand during the reductive elimination step (TS2a), where both metals are coordinated to the allyl ligand undergoing reductive elimination, may create a unique geometry that helps accelerate this step during catalysis (see TS2a). In addition, this transition states suggests that both metals share the burden of oxidation state change during reductive elimination, leading directly to formation of a diRh(II) intermediate containing a Rh-Rh bond.

For monometallic Rh(I) catalysts, we found that reductive elimination (TS1b) for the Rh(BINAP)allyl(OTFA) complex (see Table 1, entry 13) was 3.4 kcal/mol higher in energy than the corresponding beta-hydride elimination (TS2b, Figure 5c). This result supports our hypothesis that slow C–O bond reductive elimination with monometallic Rh complexes prohibits formation of the more thermodynamically favorable allylic trifluoroacetate. Instead, monometallic Rh complexes lead exclusively to the kinetically favored diene product.

In conclusion, we have demonstrated that a 2-phosphinoimidazole-derived bimetallic Rh(II) complex can enable the efficient addition of trifluoroacetate across terminal alkenes with high regioselectivity for formation of the branched secondary allylic ester. Importantly, the addition of TFA is not observed with monometallic Rh(I) complexes or bimetallic rhodium(II) tetracarboxylate complexes. Our mechanistic studies and DFT calculations suggest that reversible

hydrometallation of the allene is followed by C-O bond forming reductive elimination. This report represents a rare example of metal-catalyzed addition of weak nucleophiles to allenes.

## ASSOCIATED CONTENT

### Supporting Information

The Supporting Information is available free of charge on the ACS Publications website.

Experimental procedures and spectral information for new compounds (PDF)
X-ray crystallographic information (CIF)
Structure files for all DFT-computed transition states (.xyz)

## AUTHOR INFORMATION


### Corresponding Author

*Email: dmichaelis@chem.byu.edu


## ACKNOWLEDGMENT


We thank the United States National Science Foundation Synthesis Program for partial support of this work (CHE 1665015). Funding for Kamahao Kini-Lopes was provided by the National Science Foundation Chemistry and Biochemistry REU Site to Prepare Students for Graduate School and an Industrial Career under award CHE-2050872. We thank Brigham Young University and the Office of Research Computing, especially the Fulton Supercomputing Lab. We also thank the Simmons Research Endowment at Brigham Young University for partial funding of this work.


## REFERENCES


1. a) Blieck, R.; Taillefer, M.; Monnier, F. Metal-Catalyzed Intermolecular Hydrofunctionalization of Allenes: Easy Access to Allylic Structures via the Selective Formation of C–N, C–C, and C–O Bonds. *Chem. Rev.* **2020**, *120*, 13545–13598. b) Beccalli, E. M.; Broggini, G.; Christodoulou, M. S.; Giofrè, S. Transition Metal-Catalyzed Intramolecular Amination and Hydroamination Reactions of Allenes. In *Advances in Organometallic Chemistry*, vol 69 (2018), Elsevier inc. pp 1–71. b) Qiu, G.; Zhang, J.; Zhou, K.; Wu, J. Recent advances in the functionalization of allenes via radical process. Tetrahedron, 2018, 74, 7290–7301. c) Yu, S.; Ma, S. Allenes in Catalytic Asymmetric Synthesis and Natural Product Synthesis. *Angew. Chemie. Int. Ed.* **2012**, *51*, 3074–3112. d) Ma, S. Electrophilic Addition and Cylization Reactions of Allenes. *Acc. Chem Res.* **2009**, *42*, 1679–1688.
2. a) Yu, S.; Ma, S. How easy are the syntheses of Allenes? *Chem. Commun.* **2011**, *47*, 5384–5418. b) Kuang, J.; Ma, S.An Efficient Synthesis of Terminal Allenes from Terminal 1-Alkynes. *J. Org. Chem.* **2009**, *74*, 1763–1765.
3. Kazerouni, A. M.; McKoy, Q. A.; Blakey, S. B. Recent advances in oxidative allylic C-H functionalization via group IX-metal catalysis. *Chem. Rev.* **2020**, *56*, 12287–12300. b) Park, Y.; Kim, Y.; Chang, S. Transition Metal-Catalyzed C–H Amination: Scope, Mechanism, and Applications. *Chem. Rev.* **2017**, *117*, 9247–9301.
4. a) Hartwig, J. F. Electronic Effects on Reductive Elimination To Form Carbon–Carbon and Carbon–Heteroatom Bonds from Palladium(II) Complexes. *Inorg. Chem.* **2007**, *46*, 1936–1947. b) Racowski, J.M.; Sanford, M.S. Carbon–Heteroatom Bond-Forming Reductive Elimination from Palladium(IV) Complexes. In *Higher Oxidation State Organopalladium and Platinum Chemistry,* pp 61–84.. *Topics in Organometallic Chemistry, vol 35.* Canty, A. (eds). Springer 2011, Berlin, Heidelberg. c) Vigalok, A. Electrophilic Halogenation–Reductive Elimination Chemistry of Organopalladium and -Platinum Complexes. *Acc. Chem. Res*. **2015**, *48*, 238–247.
5. Al-Masum, M.; Yamamoto, Y. Palladium-Catalyzed Hydrocarboxylation of Allenes. *J. Am. Chem. Soc*. **1998**, *120*, 3809–3810.
6. Kim, I. S.; Krische, M. J. Iridium-Catalyzed Hydrocarboxylation of 1,1-Dimethylallene: Byproduct-Free Reverse Prenylation of Carboxylic Acids. *Org. Lett.* **2008**, *10*, 513–515.
7. a) Koschker, P.; Lumbroso, A.; Breit, B. Enantioselective Synthesis of Branched Allylic Esters via Rhodium-Catalyzed Coupling of Allenes with Carboxylic Acids. *J. Am. Chem. Soc.* **2011**, *133*, 20746–20749. b) Berthold, D.; Geissler, A. G. A.; Giofré, S.; Breit, B. Rhodium-Catalyzed Asymmetric Intramolecular Hydroamination of Allenes. *Angew. Chem. Int. Ed.* **2019**, *58*, 9994–9997. c) Hu, J.-L.; Bauer, F.; Breit, B. Ruthenium-Catalyzed Enantioselective Addition of Carboxylic Acids to Allenes. *ACS Catal.* 2021, *11*, 12301–12306.
8. Hilpert, L. J.; Breit, B. Rhodium-Catalyzed Parallel Kinetic Resolution of Racemic Internal Allenes Towards Enantiopure Allylic 1,3-Diketones. *Angew. Chem. Int. Ed.* **2019**, *58*, 9939–9943.
9. a) Ence, C.; Walker, W. K.; Martinez, E.; Stokes, R. W.; Sarager, S.; Smith, S. J.; Michaelis, D. J. "Synthesis of chiral titanium-containing phosphinoamide ligands for enantioselective heterobimetallic catalysis." Tetrahedron, 2019, 75, 3341–3347. b) Walker, W. K.; Anderson, D. L.; Stokes, R. W.; Smith, S. L.; Michaelis, D. J. Allylic Aminations with Hindered Secondary Amine Nucleophiles Catalyzed by Heterobimetallic Ti–Pd Complexes. *Org. Lett*. **2015**, *17*, 752–755. c) Walker, W. K.; Kay, B. M.; Michaelis, S. A.; Anderson, D. L.; Smith, S. J.; Ess, D. H.; Michaelis, D. J. Origin of Fast Catalysis in Allylic Amination Reactions Catalyzed by Pd–Ti Heterobimetallic Complexes. *J. Am. Chem Soc.* **2015**, *137*, 7371.
10. a) Farley, C. M.; Uyeda, C. Organic Reactions Enabled by Catalytically Active Metal-Metal bonds. *Trends Chem.* **2019**, *1*, 497–509. b) Powers, I. G.; Uyeda, C. Metal–Metal Bonds in Catalysis. *ACS Catal*. **2017**, *7*, 936–958. c) Pye, D. R.; Mankad, N. P. Bimetallic Catalysis for C–C and C–X Coupling Reactions. *Chem. Sci.* **2017**, *8*, 1705–1718. d) Cooper, B. G.; Napoline, J. W.; Thomas, C. M. Catalytic Applications of Early/Late Heterobimetallic Complexes. *Catal. Rev*. **2012**, *54*, 1–40. (e) Ritleng, V.; Chetcuti, M. J. Hydrocarbyl Ligand Transformations on Heterobimetallic Complexes. *Chem. Rev*. **2007**, *107*, 797–858.
11. Ence, C. C.; Martinez, E. E.; Himes, S. R.; Nazari, S. H.; Rodriguez Moreno, M.; Matu, M. F.; Larsen, S. G.; Gassaway, K. J.; Valdivia-Berroeta, G. A.; Smith, S. J.; Ess, D. H.; Michaelis, D. J. Experiment and Theory of Bimetallic Pd-Catalyzed α-Arylation and Annulation for Naphthalene Synthesis. *ACS. Catal.* **2021**, *11*, 10394–10404.
12. Martinez, E. E.; Rodriguez Moreno, M.; Barksdale, C. A.; Michaelis, D. J. Effect of Precatalyst Oxidation State in C–N Cross-Couplings with 2-Phosphinoimidazole-Derived Bimetallic Pd(I) and Pd(II) Complexes. *Organometallics* **2021**, *40*, 2763–2767.
13. Chipman, J. A.; Berry, J. F. Paramagnetic Metal–Metal Bonded Heterometallic Complexes. *Chem. Rev.* **2020**, *120*, 2409–2447.
14. Green, J. C.; Green, M. L. H.; Parkin, G. The occurrence and representation of three-centre two-electron bonds in covalent inorganic compounds. *Chem. Commun.* **2012**, *48*, 11481-11503.
15. a) Jurt, P.; Salnikov, O. G.; Gianetti, T. L.; Chukanov, N. V.; Baker, M. G.; Le Corre, G.; Borger, J. E.; Verel, R.; Gauthier, S.;

Fuhr, O.; Kovtunov, K. V.; Fedorov, A.; Fenske, D.; Koptyug, I. V.; Grützmacher, H. Low-valent homobimetallic Rh complexes: influence of ligands on the structure and the intramolecular reactivity of Rh–H intermediates. *Chem. Sci.* **2019**, *10*, 7937–7945. b) Weller, A. S.; McIndoe, J. S. Reversible Binding of Dihydrogen in Multimetallic Complexes. *Eur. J. Inorg. Chem.* **2007**, *28*, 4411–4423.

16. a) All structures were reoptimized from the starting crystal structure with the M06 functional using the 6-31G**[LANL2DZ for Rh] basis set in Gaussian 16. Structures were confirmed as minima or transition states by vibrational frequency analysis. Reported enthalpies correspond to 298 K and 1 atm using the standard thermochemistrycorrections in Gaussian 16. The SMD solvent model for DCE was used in all calculations. (b) Marenich, A. V.; Cramer, C. J.; Truhlar, D. G. Universal Solvation Model Based on Solute Electron Density andon a Continuum Model of the Solvent Defined by the Bulk DielectricConstant and Atomic Surface Tensions. *J. Phys. Chem. B* **2009**, *113*, 6378−6396.
17. Frisch, M. J.; Trucks, G. W.; Schlegel, H. B.; Scuseria, G. E.; Robb, M. A.; Cheeseman, J. R.; Scalmani, G.; Barone, V.; Petersson, G. A.; Nakatsuji, H.; Li, X.; Caricato, M.; Marenich, A. V.; Bloino, J.; Janesko, B. G.; Gomperts, R.; Mennucci, B.; Hratchian, H. P.; Ortiz, J. V.; Izmaylov, A. F.; Sonnenberg, J. L.; Williams; Ding, F.; Lipparini,F.; Egidi, F.; Goings, J.; Peng, B.; Petrone, A.; Henderson, T.; Ranasinghe, D.; Zakrzewski, V. G.; Gao, J.; Rega, N.; Zheng, G.; Liang, W.; Hada, M.; Ehara, M.; Toyota, K.; Fukuda, R.; Hasegawa, J.; Ishida, M.; Nakajima, T.; Honda, Y.; Kitao, O.; Nakai, H.; Vreven, T.;Throssell, K.; Montgomery, J. A., Jr.; Peralta, J. E.; Ogliaro, F.;Bearpark, M. J.; Heyd, J. J.; Brothers, E. N.; Kudin, K. N.; Staroverov,V. N.; Keith, T. A.; Kobayashi, R.; Normand, J.; Raghavachari, K.;Rendell, A. P.; Burant, J. C.; Iyengar, S. S.; Tomasi, J.; Cossi, M.;Millam, J. M.; Klene, M.; Adamo, C.; Cammi, R.; Ochterski, J. W.;Martin, R. L.; Morokuma, K.; Farkas, O.; Foresman, J. B.; Fox, D. J.Gaussian 16, Rev. B.01; Gaussian Inc.: Wallingford, CT, 2016. (b) Zhao, Y.; Truhlar, D. G. The M06 Suite of Density Functionalsfor Main Group Thermochemistry, Thermochemical Kinetics,Noncovalent Interactions, Excited States, and Transition Elements: Two New Functionals and Systematic Testing of Four M06-classFunctionals and 12 Other Functionals. *Theor. Chem. Acc.* **2008**, *120*, 215–241.
18. For selected examples, see: a) Obora, Y.; Ogawa, Y.; Imai, Y.; Kawamura, T.; Tsuji, Y. Palladium Complex Catalyzed Acylation of Allylic Esters with Acylsilanes*. J. Am. Chem. Soc.* **2001**, *123*, 10489–10493. b) Hartwig, J. F.; Pouy, M. J. Iridium-Catalyzed Allylic Substitution. In: Iridium Catalysis, Andersson, P. (eds). Topics in Organometallic Chemistry, vol 34. Springer, 2011, Berlin, Heidelberg. c) McGeough, C. P.; Strom, A. E.; Jamison, T. F. Ni-Catalyzed Cross-Electrophile Coupling for the Synthesis of Skipped Polyenes. *Org. Lett.* **2019**, *21*, 3606–3609. d) Jiang, R.; Ding, L.; Zheng, C.; You, S.-L. Iridium-catalyzed Z-retentive asymmetric allylic substitution reactions. *Science* **2021,** *371,* 380–386.
19. a) Doyle, M. P. Perspective on dirhodium carboxamidates as catalysts. *J. Org. Chem.* **2006**, *71*, 9253–9250. b) Davies, H. M. L.; Liao, K. Dirhodium tetracarboxylates as catalysts for selective intermolecular C–H functionalization. *Nature Rev. Chem.* **2019**, *3*, 347–360. c) *Rhodium Catalysis in Organic Synthesis: Methods and Reactions*; Tanaka, K. Ed.; Wiley-VCH, 2019. pp 1–667. DOI:10.1002/9783527811908.

Insert Table of Contents artwork here